New Strategy for Stark Deceleration

David Reens,* Hao Wu,† Alexander Aeppli, Anna McAuliffe, Piotr Wcisło, Tim Langen,‡ and Jun Ye
JILA, National Institute of Standards and Technology and the University of Colorado and Department of Physics, University of Colorado, Boulder, Colorado 80309-0440, USA
(Dated: January 24, 2020)

Stark deceleration is an important technology for cold and dense molecular beams, and has enabled numerous trapping and collisional studies. Nevertheless, Stark deceleration has not realized its full potential due to significant limitations in the focusing properties of Stark decelerators. We introduce a new operation strategy that resolves focusing limitations but requires no hardware modifications. We explore the physics underlying these improvements, and verify our results for hydroxyl radicals. At trappable final velocities, molecule flux improves by a factor of 4.2 ± 0.8. Improved focusing is also found to result in a recovery of gains in molecule yield with increased operating voltage. The improvement is more significant for species which require more time for deceleration, so that Stark deceleration of less readily polarized species is now more feasible.

Over the past two decades, Stark deceleration has enabled groundbreaking collisional [1–3] and spectroscopic [4–7] studies of a variety of species [8]. Subsequent trap-loading greatly enhances interrogation time for such studies [9] and opens the door for further manipulation [10]. Alongside the history of achievements enabled by Stark deceleration runs a parallel ongoing saga surrounding their efficient operation. Many important steps have been made, not only in understanding the flaws of the canonical pulsed decelerator [11, 12], but also in addressing them through the use of overtones [13, 14], undertones [15], or even mixed phase angles [16, 17]. Even with these advances, the outstanding inefficiencies of the pulsed decelerator, particularly with regard to transverse phase stability, have motivated alternative geometries such as interspersed quadrupole focusing [12] and traveling wave deceleration [18–20]. Although traveling wave deceleration takes a strong step toward truly efficient operation, it comes with significant engineering challenges. These may be partially addressed by the use of combination pulsed and traveling wave devices [21], or even using traveling wave geometry with pulsed electronics [22, 23]. In Zeeman deceleration, a parallel story has unfolded, with early demonstrations [24, 25] later improved through the use of anti-Helmholtz configurations with better transverse focusing properties [26, 27]. Lacking a comparable breakthrough for Stark devices, others have continued to pursue brand new geometries [28], or even combine the best features of Stark and Zeeman approaches in a single device [29, 30]. Our strategy works with conventional geometry and electronics, but fully resolves transverse challenges and offers gains even at very low speeds.

The strategy is to admix new field distributions into the deceleration process that feature strong restoring forces in the transverse directions. Depending on which field distributions are chosen, we specify two operating modes employing this strategy: focusing (F) and strong focusing (SF). In the conventional strategy, only two field distributions are used, and one is identical to the other up to translation and rotation. These field distributions require an electrode array with the capability to apply three distinct equally spaced voltages, usually labeled ground, plus, and minus. Both F and SF use distributions which may be generated simply by rearranging how the usual three voltages are applied to the decelerator electrodes. Although F mode is weaker, it has the unique advantage of requiring no hardware modifications, since the additional distributions may be obtained from those used conventionally by grounding electrodes that formerly would have been charged. SF mode significantly outperforms F mode in simulation, but requires all three voltages to be applied to a single electrode at different times during operation. This is something the conventional mode avoids, and is challenging to implement.

To understand the success of this new strategy, we revisit the operation of a decelerator; Fig. 1 details field distributions and the operating modes derived from them. In the conventional $S = 1$ strategy [8], low-field seeking molecules approach a charged pin pair. This process is analogous to climbing a hill, as the molecules polarize and exchange kinetic energy for internal potential energy (Fig. 1, right column). This strong field is abruptly removed by high voltage switches, before the molecules have a chance to accelerate down the hill. It is customary to discuss the behavior of an idealized "synchronous molecule" which travels along the decelerator axis with zero transverse velocity. The switching is timed so that the synchronous molecule loses an identical amount of energy at each pin pair. It is essential that the synchronous molecule travel only partway up each hill, so that molecules that are ahead of the synchronous molecule get more energy removed. This creates a longitudinal restoring force for the molecules, centered on the synchronous molecule. Transversely, restoring force is not inherited from switching events, but arises directly from the focusing properties of field distributions. We speak of these restoring forces in a time-averaged sense, where the large speed of the molecules validates the approximation that the large variation in force that all

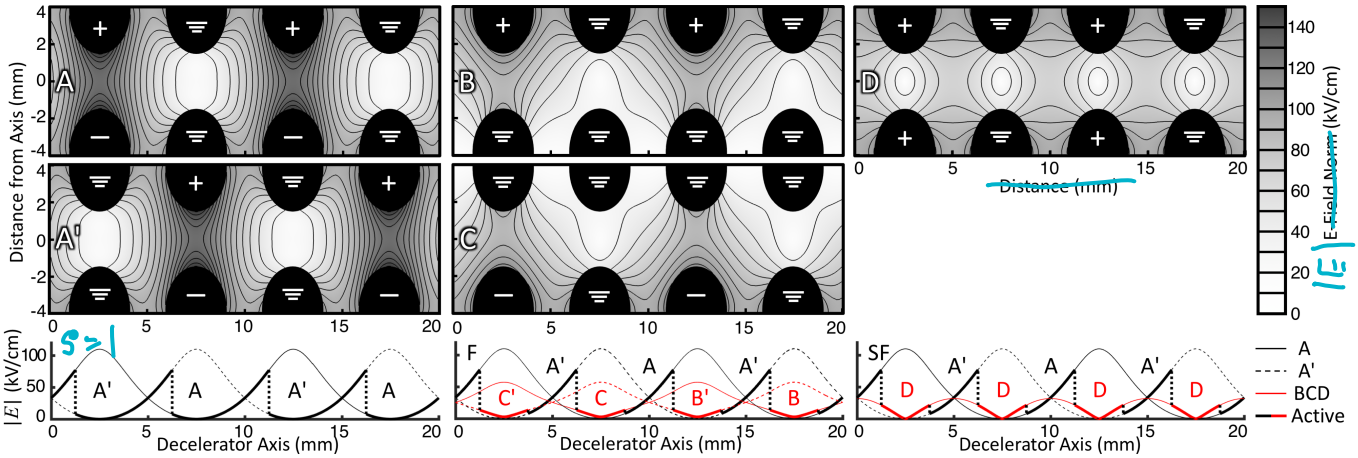

FIG. 1. A new strategy for Stark deceleration, consisting of electric field distributions with transverse focusing (above) and operation modes which employ them (below). Distributions are generated in COMSOL with 0, +12.5, or −12.5 kV applied to the pins as indicated; the chosen cut plane includes the decelerator axis and is 45° to all pins to ensure their visibility. The operation modes are specified via on-axis energy diagrams that indicate which distribution is active (bold) as a function of the synchronous molecule's position on that axis. Left: the conventional distribution A and operating mode S = 1 [13]. Prime indicates a translation of the field configuration along the axis by one pin pair, e.g. A and A′, together with a 90° rotation about that axis, since successive pin pairs are always rotated by this amount to ensure confinement in both transverse directions. Center: distributions B, C and mode F. Right: distribution D and mode SF. Distribution D shows clear focusing between grounded pin pairs near 7.5 mm, evidenced by the electric field norm increasing off axis. Distributions B, C are less visibly focusing near 7.5 mm, but after several pin pairs their average influence is focusing. Distribution A only focuses near 2.5 mm, but in fact A′ is active in this region.

molecules experience while transiting a single deceleration stage has a negligible effect compared to the average force per stage. In this approximation, these forces generate a "traveling trap" for the molecules [31], which translates along the device and decelerates according to a programmed ramp of the switching frequency.

Conventionally, pins are always charged in bipolar pairs, in which case transverse focusing occurs between the charged pin pair, but not significantly elsewhere (Fig. 1A). Molecules do not regularly access this region, since these pins must be grounded before the synchronous molecule reaches them to generate a longitudinal restoring force. Instead, the molecules then pass between grounded pins, where the transverse field is actually slightly defocusing [32]. Because of this, molecules experience a small transverse confinement on average, compared to what is possible with the field strengths typical of the decelerator. Their transverse confinement also varies with how strongly the molecules are decelerated, and with their distance from the synchronous molecule along the decelerator axis. This coupling of transverse and longitudinal confinement gives rise to the situation that molecules which are coldest longitudinally are less well confined transversely. The use of deceleration overtones (S = 3, 5, ...) [13] resolves this by allowing molecules to fully transit between charged pin pairs. This leverages the full focusing properties of the conventional field distribution, at the expense of only using 1/3 of the pin pairs for removing energy. Instead, we introduce new field distributions with strong transverse restoring forces when the synchronous molecule is between the grounded pin pair, but retain the use of the conventional distribution otherwise. Useful field distributions with transverse focusing in this region can be created by leaving these pins grounded, but charging the neighboring pins to voltages that do not sum to zero. This causes field lines to run toward the grounded pin pair, creating a focusing 2D quadrupole structure. Possibilities include charging only a single pin (Fig. 1BC, F), or charging both to the same voltage (Fig. 1D, SF).

In order to best compare these modes in a device-independent way, we perform simulations with fixed travel time (3 ms) and varying deceleration rate, see Fig. 2a. S = 1 delivers the smallest phase space volumes, although provides at least some flux even at high deceleration. Remarkably, F mode offers comparable phase space volume to S = 3, but with triple the deceleration. SF mode makes more dramatic improvements, extending significant gains to even higher decelerations than possible with any other studied modes. For the traveling wave (TW) decelerator comparison in Fig. 2, 10 kV peak to peak sine waves are assumed, to our knowledge the largest used to decelerate all the way to rest [21]. All modes besides TW use the rather small 2x2 mm^2 open area of our device, while TW devices use rings of 4 mm inner diameter. If the new modes were used with a 3×3 mm^2 [14] or a 4×4 mm^2 [33] device, phase space volume would increase approximately with the cube of pin pair spacing, and deceleration would decrease linearly since the pin-pair to pin-pair spacing also must increases. Unlike TW however, the performance of F, SF, and S = 1 all degrade below 50 m/s due to the breakdown

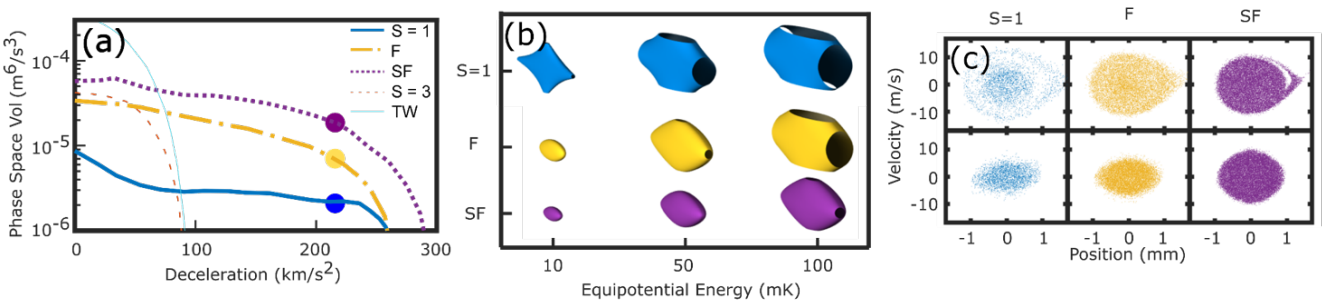

FIG. 2. Simulation results of different deceleration modes. (a) Simulated phase space volume captured by different modes of operation, for varying decelerations and elapsed time fixed at 3 ms. A 10 kV peak to peak traveling wave (TW) deceleration and ±12.5 kV S = 3 are also plotted for comparison. Three solid dots correspond to the deceleration rate used in panel (b) and (c), respectively. (b) Equipotentials of the traveling trap generated for three modes with deceleration fixed at 200 km/s^2. Lack of closure of an equipotential indicates the possibility of molecule escape. (c) Phase Space Fillings, both longitudinal (top) and transverse (bottom), for the labeled operation modes. Molecules travel for 3 ms with a deceleration of 200 km/s^2. The surviving number of molecules is 3, 11 and 24 thousand respectively. Note dramatic improvements in homogeneity and flux, without significant broadening to larger velocity classes.

of the traveling trap approximation and the discontinuous nature of pulsed deceleration.

In understanding the mechanism for this improved performance, it is helpful to visually inspect the traveling trap generated by each mode, see Fig. 2b. Here we plot equipotential surfaces for these traps at three different energies and for 200 km/s^2 deceleration. The openings in these surfaces occur when the surface reaches the 2×2 mm^2 transverse limits of our decelerator geometry. Molecules which reach this boundary encounter the surfaces of pins and are lost. Molecules may also be lost longitudinally, often remaining transversely focused but no longer decelerating with the synchronous molecule. For S = 1 mode, the 10 mK equipotential is transversely broad and even contains four small openings. This corresponds to the lack of significant transverse focusing in S = 1 for molecules close to the synchronous molecule longitudinally, which relates to the transverse-longitudinal coupling problem that has been described [11]. In general, such couplings are often useful for maintaining ergodicity in a trap [34], but with some directions featuring very low energy openings, even small amounts of motional coupling lead to loss. The improvements in operation efficiency for F and SF modes correspond to improved roundedness and tightness as evident in all equipotentials shown. This roundedness is also indicative of the independence of longitudinal and transverse focusing achieved by these modes. Molecules experience transverse restoring force regardless of their longitudinal position with respect to the synchronous molecule.

In Fig. 2c, the longitudinal and transverse phase space fillings are compared for all modes, with 200 km/s^2 deceleration and 3 ms travel time as before. All modes are initialized with the same homogeneous phase space density (PSD). This is valid when the initial beam source generates a much broader distribution than the volume accepted by the traveling trap. In the longitudinal direction, most supersonic expansions satisfy this, with the exception of those performed with a Helium buffer gas, which can reach temperatures as low as 40 mK expanding from room temperature [35]. For this work, OH expands in neon and reaches a 300 mK longitudinal temperature [36], equivalent to a velocity spread of ±17 m/s. In the transverse direction, source temperature is a more subtle phenomenon, and may be bimodal [37]. As can be seen, the distribution is nearly homogeneous after deceleration for all modes except S = 1. Apparent increases in point density between panels arise from increases in the phase space volume that is projected onto the plane. Nevertheless, these improvements can prevent reductions in PSD which stem from under filling of the phase space volume that could be subsequently utilized. For example, a trap with an acceptance comparable to the outer dimensions of the S = 1 mode will be under-filled by the S = 1 mode due to the prominent missing ring, while F mode will not do this, effectively quadrupling the phase space density loaded in such a trap. Most realistic traps possess comparable transverse and longitudinal phase space acceptances due to ergodicity, cross-dimensional couplings, or cross-dimensionally thermalizing collisions if nothing else. This makes SF mode appealing, since it delivers a phase space volume with comparable extents in both directions.

We experimentally measure the performance of F and S = 1 for hydroxyl radicals, see Fig. 3. If the distributions A, B, and C are properly arranged, F mode may be implemented from S = 1 simply by turning off one pin in a pair earlier than the other, and rotating which pin is chosen, so that even the number of required high voltage transitions is preserved between these modes. Data are collected with a beam seeded in neon and an initial speed of 825 m/s, and run times ranging from $2 - 4$ ms as the molecules are slowed close to rest. Pin spacing and most other device parameters are as previously reported [38, 39], but with increased length. S = 1 mode declines rapidly with reduced final speed, but then plateaus,

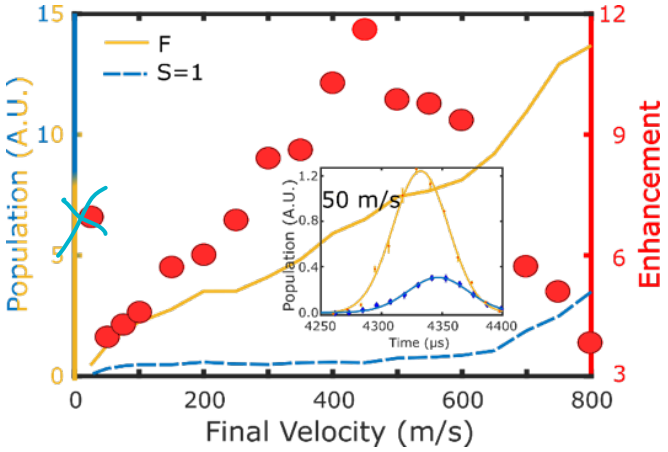

FIG. 3. The molecular signal and enhancement between F mode and conventional S=1 deceleration over a range of final speeds. Data are collected with a beam of hydroxyl radicals expanded in neon at an initial speed of 825 m/s and deceleration up to 200 km/s^2. Large gains persist at low speeds, with F outperforming S = 1 at 25 m/s by a factor of 7. The inset shows the time of flight signal from the valve pulse for F (orange) and S = 1(blue) modes measured at the end of the decelerator when slowing to 50 m/s, demonstrating a potential factor of 4 improvement at trappable final speeds.

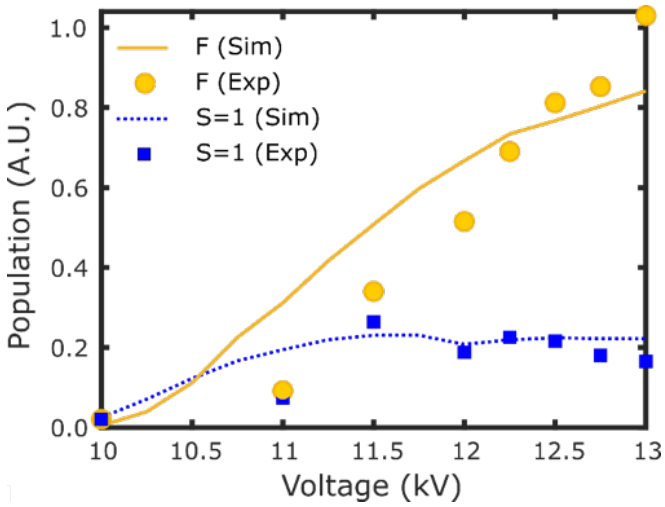

FIG. 4. Comparisons of decelerated populations between F mode and S = 1 mode at different applied voltages with a final velocity 50 m/s. The dot/square represent experimental results, which agree with the solid lines calculated from Monte Carlo simulation. Instead of showing saturation behavior as S = 1, the decelerated population using F mode increases with higher applied voltage.

indicative of the improved focusing with reduced deceleration for this mode. F mode reduces much more gradually, quadrupling S = 1 at the lowest and highest final speeds but improving by more than an order of magnitude in the central 400 − 500 m/s range. Below 50 m/s, it becomes difficult to correctly control the speed of the molecules so as to make a fair comparison, but we expect enhancements to persist and even increase as molecules benefit from a final focusing pulse applied to the very last pin pair.

To more directly validate our claim that the demonstrated improvement stems from transverse focusing, we also vary decelerator voltage. The hydroxyl radical has a linear Stark shift in our field strengths, so adjusting the voltage linearly scales the potential it experiences. For operation modes with transverse focusing that is decoupled from longitudinal, voltage increase should only improve performance, deepening the traveling trap. Fig. 4 shows the final population of molecules slowed using S = 1 and F modes to 50 m/s under different decelerator voltages. At low enough voltages, the field between the pins is not sufficient to remove enough energy per stage, and molecules cease to be decelerated. Yet at higher voltages, molecules slowed in S = 1 mode do not need to approach the pins as closely, reducing the sampling of the inter-pin focusing field. Since the F mode separates transverse focusing from slowing, molecules experience greater transverse focusing at higher field strengths. Additionally, higher fields means that molecules need a shorter period of slowing and can spend a greater amount of time in the focussing field configuration. Thus at all but the lowest field strengths F mode slowing far outperforms the conventional deceleration strategy. While in this result we were limited to 13 kV by the safety margins of our device, one may be able to see considerable efficiency gains and greater phase space acceptances at even higher voltages using these advanced modes.

We introduce a new deceleration strategy, with several accompanying modes of operation for the conventional pulsed decelerator. Significant improvements in overall performance are demonstrated. In contrast to deceleration in S = 1 mode, transverse focusing is directly applied by dedicated field distributions with much less dependence on the longitudinal coordinate, enabling further gains of performance with increased voltage. The removal of this dependence also resolves openings in the effective traveling trap which previously resulted in significant losses. This opens up possibilities for applying Stark deceleration to faster beams or to molecules with less favorable Stark shift to mass ratios, since decelerator length may be extended without suffering from increased loss due to greater time spent in traveling traps with openings. In addition to the two new operation modes identified here, a whole class of deceleration modes based upon the same strategy is ready for exploration.

* dave.reens@colorado.edu.; Present Address: Lincoln Laboratory, Massachusetts Institute of Technology, Lexington, Massachusetts 02420, USA
† Present Address: Department of Physics and Astronomy, University of California, Los Angeles, California 90095, USA
‡ Present Address: 5. Physikalisches Institut and Cen-

ter for Integrated Quantum Science and Technology (IQST), Universität Stuttgart, Pfaffenwaldring 57, 70569 Stuttgart, Germany

[1] B. C. Sawyer, B. K. Stuhl, M. Yeo, T. V. Tscherbul, M. T. Hummon, Y. Xia, J. Kłos, D. Patterson, J. M. Doyle, and J. Ye, Physical Chemistry Chemical Physics **13**, 19059 (2011).

[2] M. Kirste, X. Wang, H. C. Schewe, G. Meijer, K. Liu, A. van der Avoird, L. M. C. Janssen, K. B. Gubbels, G. C. Groenenboom, and S. Y. T. van de Meerakker, Science **338**, 1060 (2012).

[3] Z. Gao, T. Karman, S. N. Vogels, M. Besemer, A. van der Avoird, G. C. Groenenboom, and S. Y. T. van de Meerakker, Nature Chemistry **10**, 469 (2018).

[4] J. Veldhoven, J. K upper, H. L. Bethlem, B. Sartakov, A. J. A. Roij, and G. Meijer, The European Physical Journal D **31**, 337 (2004).

[5] E. R. Hudson, H. J. Lewandowski, B. C. Sawyer, and J. Ye, Physical Review Letters **96**, 143004 (2006).

[6] B. L. Lev, E. R. Meyer, E. R. Hudson, B. C. Sawyer, J. L. Bohn, and J. Ye, Physical Review A **74**, 061402 (2006).

[7] A. Fast, J. E. Furneaux, and S. A. Meek, Physical Review A **98**, 052511 (2018).

[8] S. Y. T. van de Meerakker, H. L. Bethlem, N. Vanhaecke, and G. Meijer, Chemical Reviews **112**, 4828 (2012).

[9] B. C. Sawyer, B. K. Stuhl, D. Wang, M. Yeo, and J. Ye, Physical Review Letters **101**, 203203 (2008).

[10] D. Reens, H. Wu, T. Langen, and J. Ye, Physical Review A **96**, 063420 (2017).

[11] S. Y. T. van de Meerakker, N. Vanhaecke, and G. Meijer, Annual Review of Physical Chemistry **57**, 159 (2006).

[12] B. C. Sawyer, B. K. Stuhl, B. L. Lev, J. Ye, and E. R. Hudson, European Physical Journal D **48**, 197 (2008).

[13] S. Y. T. van de Meerakker, N. Vanhaecke, H. L. Bethlem, and G. Meijer, Physical Review A **71**, 053409 (2005).

[14] L. Scharfenberg, H. Haak, G. Meijer, and S. Y. T. van de Meerakker, Physical Review A **79**, 023410 (2009).

[15] D. Zhang, G. Meijer, and N. Vanhaecke, Physical Review A **93**, 023408 (2016).

[16] L. P. Parazzoli, N. Fitch, D. S. Lobser, and H. J. Lewandowski, New Journal of Physics **11**, 055031 (2009).

[17] S. Hou, S. Li, L. Deng, and J. Yin, Journal of Physics B: Atomic, Molecular and Optical Physics **46**, 045301 (2013).

[18] A. Osterwalder, S. A. Meek, G. Hammer, H. Haak, and G. Meijer, Physical Review A **81**, 051401 (2010).

[19] J. van den Berg, S. Mathavan, C. Meinema, J. Nauta, T. Nijbroek, K. Jungmann, H. Bethlem, and S. Hoekstra, Journal of Molecular Spectroscopy **300**, 22 (2014).

[20] M. I. Fabrikant, T. Li, N. J. Fitch, N. Farrow, J. D. Weinstein, and H. J. Lewandowski, Physical Review A **90**, 033418 (2014).

[21] M. Quintero-Pérez, P. Jansen, T. E. Wall, J. E. van den Berg, S. Hoekstra, and H. L. Bethlem, Physical Review Letters **110**, 133003 (2013).

[22] S. Hou, Q. Wang, L. Deng, and J. Yin, Journal of Physics B: Atomic, Molecular and Optical Physics **49**, 065301 (2016).

[23] Y. Shyur, J. A. Bossert, and H. J. Lewandowski, Journal of Physics B: Atomic, Molecular and Optical Physics **51**, 165101 (2018).

[24] N. Vanhaecke, U. Meier, M. Andrist, B. H. Meier, and F. Merkt, Phys. Rev. A **75**, 31402 (2007).

[25] E. Narevicius, A. Libson, C. G. Parthey, I. Chavez, J. Narevicius, U. Even, and M. G. Raizen, Physical Review Letters **100**, 093003 (2008).

[26] E. Lavert-Ofir, S. Gersten, A. B. Henson, I. Shani, L. David, J. Narevicius, and E. Narevicius, New Journal of Physics **13**, 103030 (2011).

[27] K. Dulitz, M. Motsch, N. Vanhaecke, and T. P. Softley, The Journal of Chemical Physics **140**, 104201 (2014).

[28] Q. Wang, S. Hou, L. Xu, and J. Yin, Physical Chemistry Chemical Physics **18**, 5432 (2016).

[29] T. Cremers, S. Chefdeville, N. Janssen, E. Sweers, S. Koot, P. Claus, and S. Y. T. van de Meerakker, Phys. Rev. A **95**, 43415 (2017).

[30] V. Plomp, Z. Gao, T. Cremers, and S. Y. T. van de Meerakker, Physical Review A **99**, 33417 (2019).

[31] H. L. Bethlem, G. Berden, A. J. A. van Roij, F. M. H. Crompvoets, and G. Meijer, Physical Review Letters **84**, 5744 (2000).

[32] This is not highly apparent in Fig. 1b-A, where a 45° slicing plane is chosen for visual clarity. The defocusing is strongest in the plane including the decelerator axis that is also normal to the cylindrical axis of the grounded pins.

[33] S. Y. T. van de Meerakker, P. H. M. Smeets, N. Vanhaecke, R. T. Jongma, and G. Meijer, Physical Review Letters **94**, 023004 (2005).

[34] E. L. Surkov, J. T. M. Walraven, and G. V. Shlyapnikov, Physical Review A **53**, 3403 (1996).

[35] U. Even, Advances in Chemistry **2014**, 636042 (2014).

[36] H. Wu, D. Reens, T. Langen, Y. Shagam, D. Fontecha, and J. Ye, Physical Chemistry Chemical Physics **20**, 11615 (2018).

[37] H. Beijerinck and N. Verster, Physica B+C **111**, 327 (1981).

[38] J. R. Bochinski, E. R. Hudson, H. J. Lewandowski, and J. Ye, Physical Review A **70**, 043410 (2004).

[39] B. C. Sawyer, B. L. Lev, E. R. Hudson, B. K. Stuhl, M. Lara, J. L. Bohn, and J. Ye, Physical Review Letters **98**, 253002 (2007).